



Influence of relative humidity on aerosol composition: Impacts on light extinction and visibility impairment at two sites in coastal area of China

W.J. Qu^{a,*}, J. Wang^b, X.Y. Zhang^c, D. Wang^d, L.F. Sheng^a

^a Physical Oceanography Laboratory, Key Laboratory of Ocean–Atmosphere Interaction and Climate in Universities of Shandong, Ocean University of China, Qingdao 266100, China

^b Department of Earth and Atmospheric Sciences, University of Nebraska-Lincoln, Lincoln, NE 68588-0340, USA

^c Key Laboratory for Atmospheric Chemistry, Chinese Academy of Meteorological Sciences, CMA, 46 Zhong Guan Cun S. Ave., Beijing 100081, China

^d State Key Laboratory of Loess and Quaternary Geology, Institute of Earth Environment, Chinese Academy of Sciences, 10 Fenghui S. Rd., PO Box 17, XiAn 710075, China

ARTICLE INFO

Article history:

Received 3 June 2014

Received in revised form 16 September 2014

Accepted 9 October 2014

Available online 23 October 2014

Keywords:

Atmospheric aerosol
Mass extinction efficient
Sulfate fraction
Visibility
Coastal China

ABSTRACT

Investigation on the aerosol characteristics, surface visibility (Vis) and meteorology at BGS (Baguanshan, Qingdao) and LNA (Lin'an, Zhejiang) shows that the ambient aerosol chemical composition and light extinction are relative humidity (RH) dependent. At higher RH, both the strengthened hygroscopic growth and the more efficient oxidization (of the precursor gases and formation of the secondary sulfate and nitrate) contribute to the increase of the mass fraction of the hygroscopic species, which consequently results in the increase of the aerosol mass extinction efficiency (MEE) and Vis reduction at the two Chinese coastal sites. MEE and chemical composition of the aerosol vary significantly under different regional transport ways; the airmasses from the ocean directions are associated with higher RH, higher sulfate mass fraction and greater MEE at BGS, while MEEs are smaller and associated with lower RH and lower sulfate fraction for the airmasses from the continent directions. Vis shows better correlation with PM_{2.5} and PM₁₀ mass concentrations when RH effect on aerosol hygroscopic growth is considered. At BGS, the sulfate mass fraction in PM_{2.5} and PM₁₀ (in average 32.4% and 27.4%) can explain about 60.7% and 74.3% of the variance of the aerosol MEE, respectively; sulfate and nitrate contribute to about 61% of the light extinction. RH plays a key role in aerosol extinction and visibility variation over this coastal area of China. Formation of the secondary aerosol (especially sulfate and nitrate) as well as hygroscopic growth under favorable (more stable and humid) meteorological conditions should be paid adequate attention in regulation of air quality and Vis improvement over eastern China in addition to the routine emission control measurements.

© 2014 Elsevier B.V. All rights reserved.

1. Introduction

Increase in energy consumption along with urbanization and industrialization has led to more frequent air pollution episodes (Chan and Yao, 2008) and low visibility (Vis) events in

China (Qiu and Yang, 2000; Fan et al., 2005; Che et al., 2007; Deng et al., 2008; Chang et al., 2009), which have raised worldwide concern (Tao et al., 2012; Zhao et al., 2013). Although a lot of efforts have been implemented to improve air quality as well as to control the occurrence of fog and haze events in China, the effects of these measurements (without full understanding and consideration of the weather and climate background of the recently accelerated intensification of these severe haze and fog events) are mostly limited. A key challenge that still remains is to find and pay adequate attention

* Corresponding author at: Physical Oceanography Laboratory, Ocean University of China, Qingdao 266100, China. Tel.: +86 532 66781309; fax: +86 532 66782790.

E-mail addresses: quwj@ouc.edu.cn, quwj@163.com (W.J. Qu).

to the major contributors to the aerosol extinction and Vis impairment during these typical air pollution episodes over the region.

It is well known that the hygroscopic growth of the aerosol affects its optical characteristic (such as the single-scattering albedo and the refractive index; Zieger et al., 2013) and size distribution, which have important implications to the radiative forcing (Chýlek et al., 1995; Kotchenruther et al., 1999; Wang et al., 2008; Rastak et al., 2014) and the variation of Vis (Noll et al., 1968; Charlson, 1969). Aerosol hygroscopicity is also important for accurate satellite retrieval (Wang and Martin, 2007). A recent study over eastern China (ECN) found that in addition to emission, the relative humidity (RH) is an important meteorological factor (except for the wind speed and regional transport of the pollutants) contributing to the variation of Vis (Qu et al., 2014), and regional statistics for the 136 stations show that RH is strongly correlated with the detrended Vis (calculated through subtracting the linear trend from the original time series of Vis) in winter over ECN from 1973 to 2012 ($R = -0.81$, $P < 0.0001$, $n = 40$); higher RH and more humid environment are found to be more favorable for the hygroscopic growth of the particles and subsequently Vis decline.

Along the same line, increase of the aerosol optical depth (AOD) is found to be associated with increase of the total column water vapor content (CWV, Smirnov et al., 2002; Eck et al., 2008). Bi et al. (2014) found a strong positive correlation between AOD and CWV at Beijing during the severe haze episodes in January 2013, and they attributed the large accumulation mode particles then to the coagulation through both condensation and gas-to-particle conversion processes. Through comparison of the dry and ambient aerosol light extinction coefficient (B_{ext}), Jung et al. (2009a) estimated the contribution of the aerosol water content to light extinction. The aerosol water content was found to contribute significantly to the light extinction (about 51.4% and 68.4% during the biomass burning and the long-range transport periods) under Asian continental outflow (Jung and Kim, 2011). Jung et al. (2009a) further found that the effect of aerosol water content on Vis impairment and light extinction is mainly due to increases of the $(\text{NH}_4)_2\text{SO}_4$ and NH_4NO_3 concentrations in the Pearl River Delta region.

Indeed, Li et al. (2013) reported that the chemical composition of the aerosol has an influence on its optical properties (especially the single scattering albedo) in urban Shanghai. Sulfate is found to be a major aerosol species contributing to Vis reduction in USA (Malm et al., 1994). A study in Beijing found that sulfate, nitrate and organic carbon mass contributed to about 42.2%, 24.9% and 15.7%, respectively, of light extinction in summer 2006 (Jung et al., 2009b). On the other hand, the formation of secondary hygroscopic aerosol (such as SO_4^{2-} , NO_3^- , and NH_4^+) is found to be an important mechanism of haze over Beijing (Zhao et al., 2013). Secondary pollutants including the hygroscopic species were the major chemical components during haze days in Guangzhou (Tan et al., 2009). Sun et al. (2014) also reported that the secondary inorganic species play enhanced roles in the haze formation and their contributions elevated during haze episodes in Beijing in January 2013. Furthermore, RH is found to have important impacts on aerosol composition (especially sulfate and coal combustion organic aerosol) during winter in Beijing (Sun et al., 2013).

How does RH influence the chemical composition and optical properties of the aerosol (and consequently contribute to Vis degradation)? As RH and water vapor are important to light extinction and AOD, what is the impact of the variation in water vapor supply and RH under different regional atmospheric transport ways to aerosol extinction and Vis impairment? Further clarifying these questions in coastal area of China is important to air quality regulation and Vis improvement measurements over the region.

Here we use observations of surface Vis and meteorology as well as measurements of aerosol mass concentration and chemical composition at two sites over coastal China to investigate the RH influences on aerosol composition, extinction and Vis variation. The enhanced aerosol extinction is linked with the increase of the mass fraction of sulfate and nitrate at elevated RH. Both the RH effects on formation of the secondary species and on hygroscopic growth are considered. The results of this study will be helpful to better understand the effect of meteorology (in this case RH variation) on the light extinction of aerosol and Vis decline over the coastal area of China.

2. Data and method

2.1. Sampling and chemical analysis of PM

Measurements of aerosol mass concentration and chemical composition were conducted during a year-round campaign at two sites: (1) Baguanshan (BGS, $36^\circ 04' \text{ N}$, $120^\circ 20' \text{ E}$, 76 m above sea level) in a residence district of Qingdao, a coastal city; (2) Lin'an (LNA, $30^\circ 17' \text{ N}$, $119^\circ 44' \text{ E}$, 138 m asl), a rural site in the east of the Plain of Yangtze River Middle and Lower Reaches. The two sites are located in ECN (with the Yellow Sea or the East China Sea to the east and mainland China to the west), a region with dense population, upgrowth industry, and significant anthropogenic emissions. In summer, East Asian summer monsoon is the major synoptic system with humid climate; in spring there is input of Asian dust to the region.

Bulk 24-h (from 9:00 AM to 9:00 AM the next day) $\text{PM}_{2.5}$ and PM_{10} (particulate matter with diameter less than 2.5 μm and 10 μm) samples were collected every other day from May 2007 to June 2008 at BGS with a MiniVol™ air sampler (Airmetrics, Oregon USA) operating at a flow of 5 l min^{-1} . At LNA, bulk 24-h (9:10 AM to 9:10 AM the next day) $\text{PM}_{2.5}$ samples were collected from March 2004 to June 2005 with an R&P 2025 sampler (Rupprecht & Patashnick, USA) at a flow rate of 16.7 l min^{-1} ; except for sampler maintenance, from March 3, 2004 to January 11, 2005 one sample was collected every other day, while from January 12 to June 8, 2005 one sample was collected every day.

Aerosol particles were collected on 47 mm diameter Whatman quartz microfibre filters (QM/A, Whatman Ltd, Maidstone, UK) (preheated at 800 °C for 4 h to remove contaminants). The filter samples were equilibrated for at least 24 h under a constant RH between 30% and 40%, then aerosol mass was determined gravimetrically using an electronic microbalance with 1 μg sensitivity (ME 5-F, Sartorius AG, Goettingen Germany), which is referred to as dry mass in this study. Samples were stored in a refrigerator at 4 °C before chemical analysis.

The analytical techniques used have been described previously (Qu et al., 2008). Chemical analyses of the water-soluble ions, including SO_4^{2-} , NO_3^- , NH_4^+ , Ca^{2+} , Mg^{2+} , K^+ , Na^+ , NO_2^- , Cl^- and F^- , were conducted using a Dionex® 600 ion

chromatograph (IC) equipped with an ED50A electrochemical detector (Dionex Corp, Sunnyvale, CA, US). Concentrations of trace elements were determined by a proton-induced X-ray emission (PIXE) method; eighteen elements were analyzed but only the concentration of Fe was used here to estimate the contribution of mineral dust aerosol. All data were corrected for backgrounds from the average of blank filters.

2.2. Vis, meteorological data and MEE

Vis and meteorological data are extracted from the Global Summary of Day (GSOD) database (<ftp://ftp.ncdc.noaa.gov/pub/data/g sod>), which has undergone extensive automated quality control and been widely used (Chang et al., 2009; Wang et al., 2009). The horizon Vis is derived from the visual range measured by professional observers using reference objects at known distances. Daily Vis was estimated by averaging the observations (for the day with at least four records) with an uncertainty of 0.1 km (China Meteorological Administration, 2003).

Not available at LNA, the Vis and meteorological data at Hangzhou (a city about 50 km east) are used to study the relationship with aerosol concentration and composition (obtained at LNA). Hence as expected, the result at LNA is not ideal as it should be.

The mass extinction efficiency (MEE) of aerosol, defined as the ratio of the extinction coefficient to the (dry) PM mass concentration (Si et al., 2005), is also computed. Here the light extinction coefficient (B_{ext}) is derived from Vis based upon Koschmieder's formula:

$$B_{\text{ext}} = 3.912/V, \quad (1)$$

where B_{ext} is the volume extinction coefficient and V denotes Vis (in km).

Note that Vis shows exponential decay with the increase of MEE (will be discussed in Section 3.6 and illustrated in Fig. 8); high MEE is generally associated with low Vis.

2.3. Trajectory cluster

The aerosols were also categorized into different transport clusters to evaluate the extinction at BGS (Fig. 1, Section 3.5.). Three-day airmass backward trajectories (four times each day, 00:00, 06:00, 12:00 and 18:00 UTC) were calculated with the NOAA HYSPLIT4 trajectory model (Draxler and Hess, 1998) by using the NCEP (National Center for Environmental Prediction) final analysis meteorological data. Because of the relatively simple and flat plain topography in the nearby region, the end points for the trajectories were set to 500 m above surface at BGS. The trajectories were divided into distinct clusters by using a trajectory clustering method (Arimoto et al., 1999); squared Euclidean distances were used to determine the similarities between trajectories and Ward's method was used to make hierarchical cluster.

3. Results and discussion

3.1. Ion balance of the aerosol and its implication

Ion balance evaluation has been used to check the speciation data and to find the probably undetected ion species (Jain et al., 2000; Zhang et al., 2002). The anion and cation equivalences (micro-equivalents per cubic meter, $\mu\text{eq m}^{-3}$) were calculated as:

$$\text{Anion equivalence } (\mu\text{eq m}^{-3}) = [\text{F}^-] + [\text{Cl}^-] + [\text{NO}_2^-] + [\text{SO}_4^{2-}] + [\text{NO}_3^-] \quad (2)$$

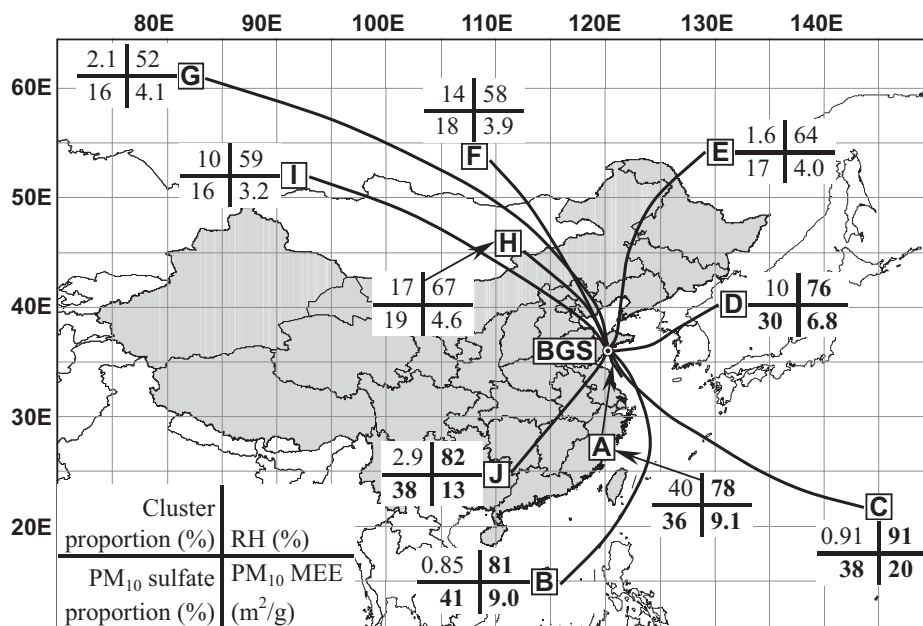


Fig. 1. Location and 3-day backward trajectory clusters for BGS (Clusters A–J). China continent is shaded with gray. The proportion of the trajectories belongs to each specific cluster in all the trajectories, the mean relative humidity (RH), sulfate (SO_4^{2-}) proportion in PM_{10} and PM_{10} mass extinction efficiency (MEE) for the trajectory clusters are also presented; boldface indicated RH, sulfate proportion and MEE for the trajectory clusters with mean RH >70%.

$$\begin{aligned} \text{Cation equivalence } (\mu\text{eq m}^{-3}) \\ = [\text{Na}^+] + [\text{NH}_4^+] + [\text{K}^+] + [\text{Mg}^{2+}] + [\text{Ca}^{2+}]. \end{aligned} \quad (3)$$

Fig. 2 shows that the cation equivalence is in deficit to neutralize the anions at BGS and LNA, reflecting the characteristic of an acidic air pollution aerosol (Maxwell-Meier et al., 2004). The ion imbalance (cation equivalence minus anion equivalence) is found to be negatively correlated with PM mass concentration ($R^2 = 0.223$ and 0.102 , $n = 157$, $P < 0.0001$ for $\text{PM}_{2.5}$ and PM_{10} at BGS, $R^2 = 0.327$, $n = 200$, $P < 0.0001$ for $\text{PM}_{2.5}$ at LNA) and positively correlated with Vis ($R^2 = 0.240$ and 0.144 , $n = 157$, $P < 0.0001$ for $\text{PM}_{2.5}$ and PM_{10} at BGS, $R^2 = 0.0605$, $n = 200$, $P < 0.0005$ for $\text{PM}_{2.5}$ at LNA). The more negative value of the ion imbalance (i.e., the more acidic aerosol) is associated with higher PM mass concentration and lower Vis, which reflects the nature of an acidic pollution air and that aerosol in the more polluted air is more acidic, implying the increase of the sulfate and nitrate during the regional air pollution episodes.

As introduced in Section 2.1, anthropogenic emissions are significant in this region. The anthropogenic secondary particles (i.e., sulfate, nitrate and other components) are found to be mainly enriched in the fine mode, while Na^+ , Mg^{2+} , Ca^{2+} and other alkaline cations which can neutralize the anions are mainly presented in coarse mode (Krivacsy and Molnar, 1998); this probably has resulted in higher anion equivalence at BGS and LNA. These ion balance results are consistent with the high frequency of acid rain (97.5%) and the low pH of precipitation (4.04) in Lin'an (Lin et al., 2004). The similar deficit of cation equivalence was also reported for aerosol over the Yellow Sea and the Bohai Sea (Xue et al., 2011). The simulated high concentrations of sulfate and nitrate over the coastal areas of China (Ge et al., 2011) are also consistent with our result here.

3.2. Variation of Vis and its relationship with PM and RH

Fig. 3 clearly shows that low Vis is generally associated with high PM concentration and high RH (marked by dash vertical lines), while high Vis is generally associated with low PM concentration and low RH (marked by dot dash vertical lines) at BGS. This is also true for variations of Vis, RH and $\text{PM}_{2.5}$ mass concentration at LNA. Details about relationship between $\text{PM}_{2.5}$, PM_{10} and their major components are also provided in Supplementary material 1.

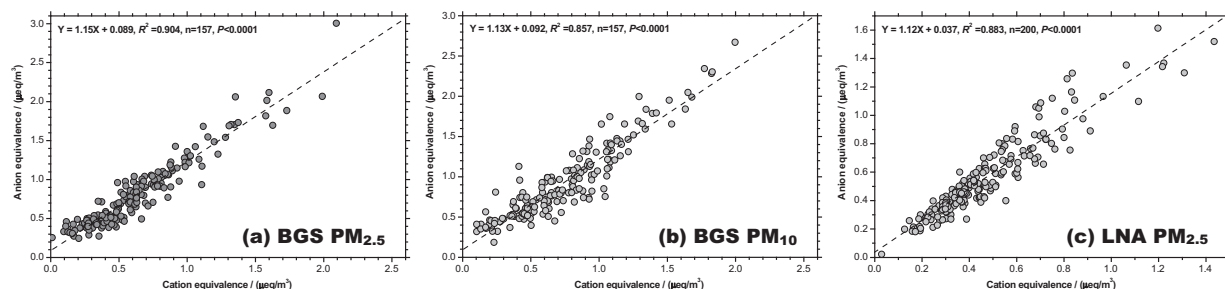


Fig. 2. Ion balance evaluation between water-soluble cations and anions in (a) $\text{PM}_{2.5}$, (b) PM_{10} at BGS and (c) $\text{PM}_{2.5}$ at LNA. The equivalence of the cations is generally in deficit to neutralize the anions at both sites, reflecting the characteristic of slightly acidic pollution aerosol (Maxwell-Meier, 2004).

To address the effect of hygroscopic growth, the RH corrected PM concentration is calculated from the dry PM concentration (gravimetrically determined in the laboratory) according to the formula " $r(\text{RH})/r(\text{dry}) = (1-\text{RH})^{-1/\mu}$, $\mu = 4.4$ for the polluted atmospheric particles (Kasten, 1969; Sun, 1985)." Here $r(\text{RH})$ is the radius of the (swelling) particle under the ambient RH, $r(\text{dry})$ is the radius of the dry particle; and the densities of the swelling and dry particles are assumed identical. A moderate correlation is found between Vis and the dry PM concentration on all weather days ($R^2 = 0.323$ and 0.285 for $\text{PM}_{2.5}$ and PM_{10} at BGS; $R^2 = 0.194$ for $\text{PM}_{2.5}$ at LNA). In contrast, a better correlation is found between Vis and the RH corrected PM concentration on all weather days (Fig. 4b, d and f), and this correlation is even better than that between Vis and the dry PM concentration only on clear days (Fig. 4a, c and e). Hence hygroscopic growth is an important factor affecting the Vis–PM relationship. More analysis on Vis in different PM and RH bins follows in Section 3.6.

3.3. Variation of the mass fraction of aerosol components with RH

Sulfate (SO_4^{2-}) mass fraction in PM shows an exponential growth accompanied with the increase of RH (Fig. 5a and b). Similarly, the nitrate (NO_3^-) proportion in PM_{10} also increases with the increase of RH (positive correlation, $R^2 = 0.157$, $n = 157$, $P < 0.0001$). Such an increase of the sulfate and nitrate fraction at elevated RH is consistent with the negative correlation between the ion imbalance and RH ($R^2 = 0.113$ and 0.0729 , $n = 157$, $P < 0.0001$ for $\text{PM}_{2.5}$ and PM_{10} at BGS); that is, the more negative ion imbalance (i.e., more acidic aerosol) is associated with higher RH, suggesting that the more humid condition tends to be favorable for the formation of more acidic aerosol (probably due to increased contribution from sulfate and nitrate). Combined with the results in Section 3.1, the more negative ion imbalance (and the more acidic aerosol) is associated with higher PM mass, lower Vis and higher RH, which is probably a result of enhanced oxidization of the precursor gases and formation of the secondary sulfate and nitrate at elevated RH.

Indeed, Pu and Yang (2000) have reported that water content of the aerosol (which is associated with the ambient RH) is essential for the oxidization of sulfur dioxide and nucleation of sulfate (in which water vapor serves as a source of the hydroxyl radical (OH), Seinfeld and Pandis, 2006), and the acidification of aerosol tends to be of more extent under high RH condition. Sun et al. (2013) also reported the significant impact of liquid water on sulfate production at high RH levels

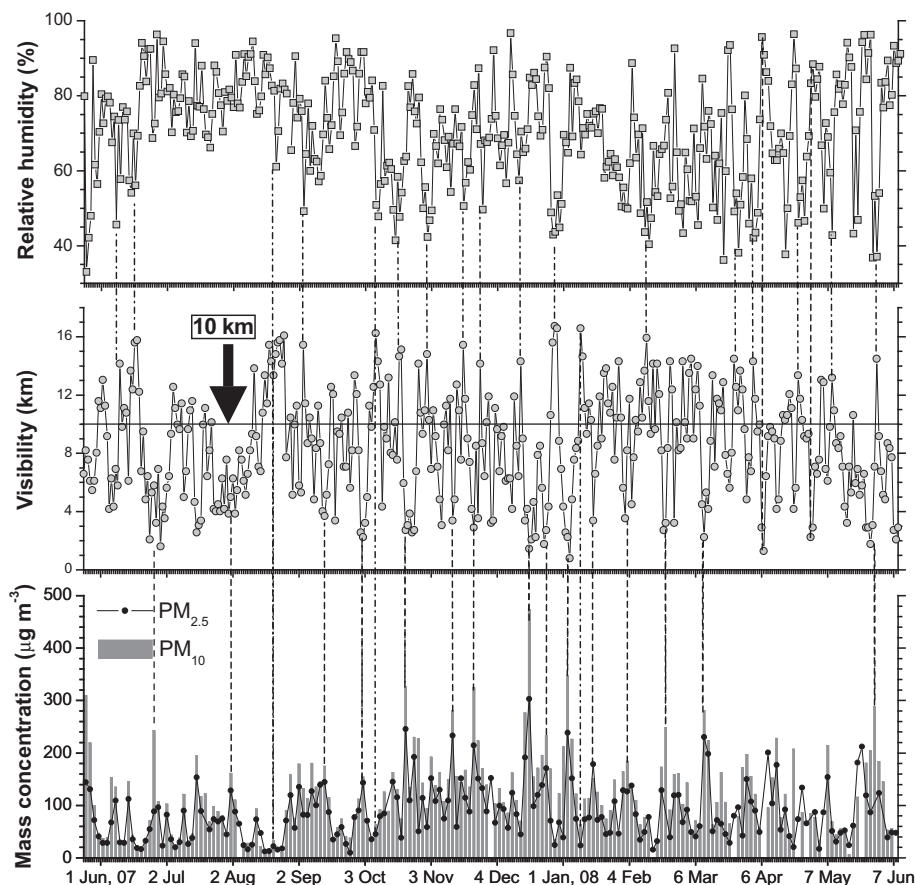


Fig. 3. Time series of (top) ambient relative humidity (RH), (middle) horizon visibility (Vis), (bottom) $PM_{2.5}$ and PM_{10} mass concentration at BGS from May 2007 to June 2008. The solid horizon line in the middle panel indicates the Vis equal to 10 km, the minimum value for Vis to be graded as “fine” at a given day (China Meteorological Administration, 2010). The dash vertical lines indicate the low Vis days, generally corresponding to high PM concentration and high RH. The dot dash vertical lines indicate the high Vis days, generally corresponding to low PM concentration and low RH.

(>50%). These studies support our conclusion here that the more humid condition favors the formation of secondary sulfate. Such RH effect on the oxidation of sulfur dioxide and acidification of the aerosol probably has important implications to light extinction and potential acid deposit over this coastal area of China.

As a major component, sulfate (SO_4^{2-}) accounts for 32.4% and 27.4% of $PM_{2.5}$ and PM_{10} masses at BGS, and 28.9% of $PM_{2.5}$ mass at LNA. As higher RH over this coastal area is favorable for the formation of sulfate and nitrate, controlling emissions of the precursor gases such as SO_2 and NO_x is still an important strategy for Vis and air quality improvement over the coastal area of China, even if the occurrence of fog and haze (mostly due to favorable stable meteorology) is more difficult to be reduced artificially.

On the contrary, dust proportion in PM shows an exponential decay as RH increases (Fig. 5c and d), which is possibly due to more efficient wet scavenging under high RH conditions, but may also reflect seasonal co-variation of RH and dust aerosol. While dust contribution to the total aerosol is less in summer and autumn (when RH at a higher level), its contribution becomes more important in spring and winter (when RH is lower). Here dust concentration is estimated from elemental Fe

which is found to account for 4% of Asian dust (Zhang et al., 2003).

3.4. Relationship of MEE with RH, PM and the mass fraction of aerosol components

MEE is found to be mass and RH dependent; it shows exponential decay with the increase of PM mass concentration (Fig. 6d, e and f) and exponential growth with the increase of RH (Fig. 6a, b and c); probably reflecting the enhanced light scattering due to the increased fraction of sulfate and nitrate as discussed in Section 3.3). The threshold values in Fig. 6 indicate the sensitive areas within which MEE responds more efficiently with the change of PM concentration and RH, similar as the results in Qu et al. (2013).

Accompanied with the increase of RH, similar increase is found for MEE (Fig. 6a, b and c) and the sulfate proportion (Fig. 5a and b). Furthermore, there is a positive correlation between MEE and the sulfate proportion (Fig. 7a, b and c), in which the sulfate proportion can explain about 60.7% and 74.3% of the variance of MEE for $PM_{2.5}$ and PM_{10} at BGS, and about 30.6% of the MEE variance for $PM_{2.5}$ at LNA (MEE derived from Vis at Hangzhou but $PM_{2.5}$ obtained at LNA). In addition, a

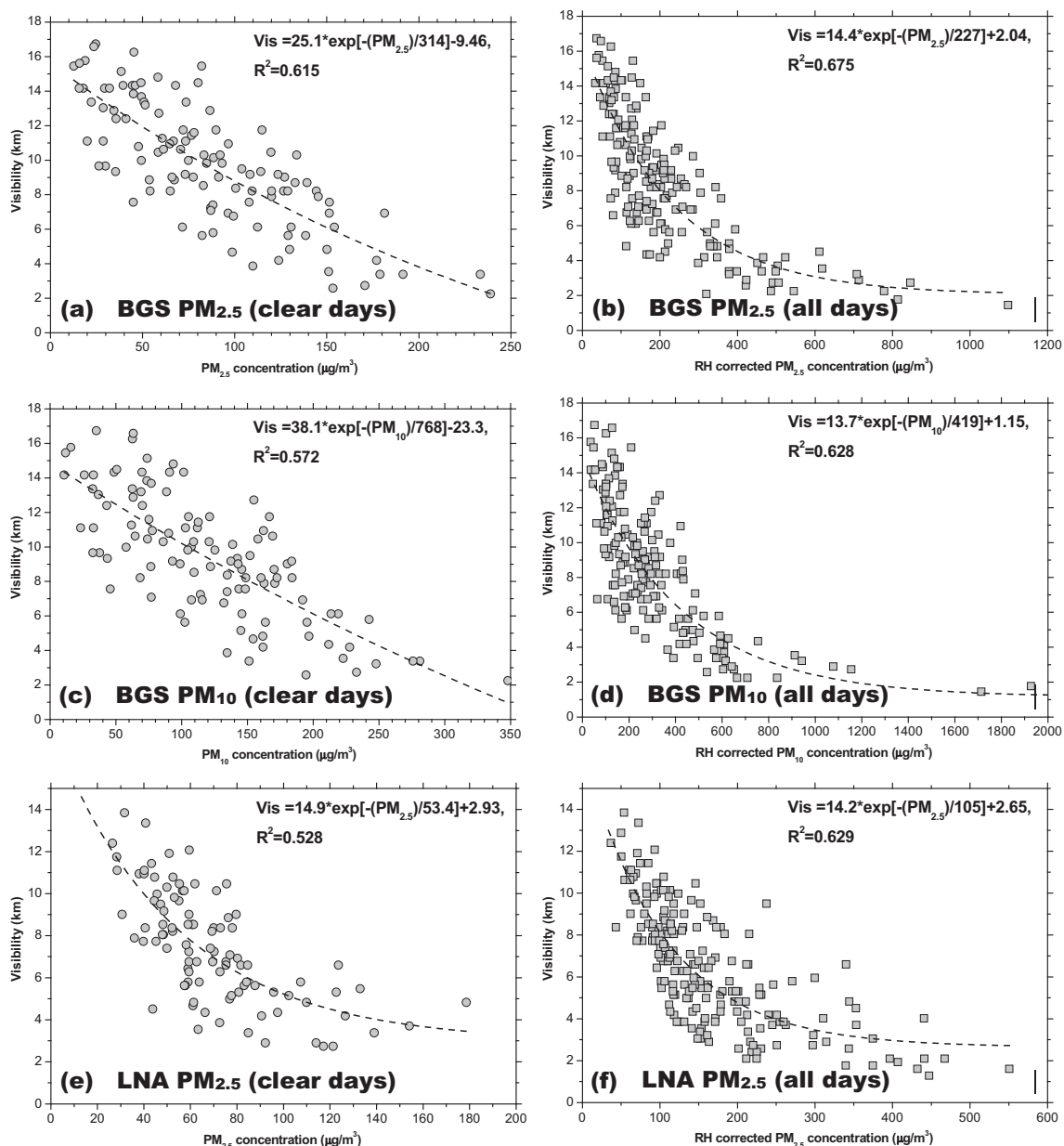


Fig. 4. The relationship between visibility (Vis) with (a) dry $PM_{2.5}$ mass concentration on clear days and (b) RH corrected $PM_{2.5}$ mass concentration on all weather days at BGS; (c), (d), same as (a), (b) but for PM_{10} ; (e), (f), same as (a), (b) but for $PM_{2.5}$ at LNA. RH corrected PM mass concentration is calculated according to the relationship of the radii of the swelling and dry particles " $r(RH)/r(dry) = (1-RH)^{-1/\mu}$, $\mu = 4.4$ for the polluted atmospheric particles" (Kasten, 1969; Sun, 1985) and assuming the densities of the swelling and dry particles are identical.

positive correlation is also identified between MEE and the nitrate proportion ($R^2 = 0.226$ and 0.360 , $n = 157$, $P < 0.0001$ for $PM_{2.5}$ and PM_{10} at BGS). As the sulfate and nitrate fractions increase at elevated RH (discussed in Section 3.3), increase of the ambient aerosol extinction efficiency (as well as decrease of Vis) is thus associated with increase of the major hygroscopic components (such as sulfate and nitrate probably due to the enhanced oxidation and formation of secondary sulfate/nitrate) as RH increases in this coastal area of China. This result is consistent with Yoon and Kim (2006) which reported enhancement of aerosol extinction and scattering with the

increase of RH, also consistent with Jung et al. (2009a) which found that the effect of aerosol water content on Vis impairment and light extinction is mainly due to increases of the $(NH_4)_2SO_4$ and NH_4NO_3 concentrations.

Contrary to the increase of MEE associated with the increase of the sulfate and nitrate fraction (Fig. 7a, b, c and discussion above), MEE shows exponential decay with the increase of dust proportion (Fig. 7d and e). These results are similar as those of Day and Malm (2001) that higher fractions of soluble inorganic compounds (sulfate and nitrate) produce growth curves of greater magnitude than do higher concentrations of either

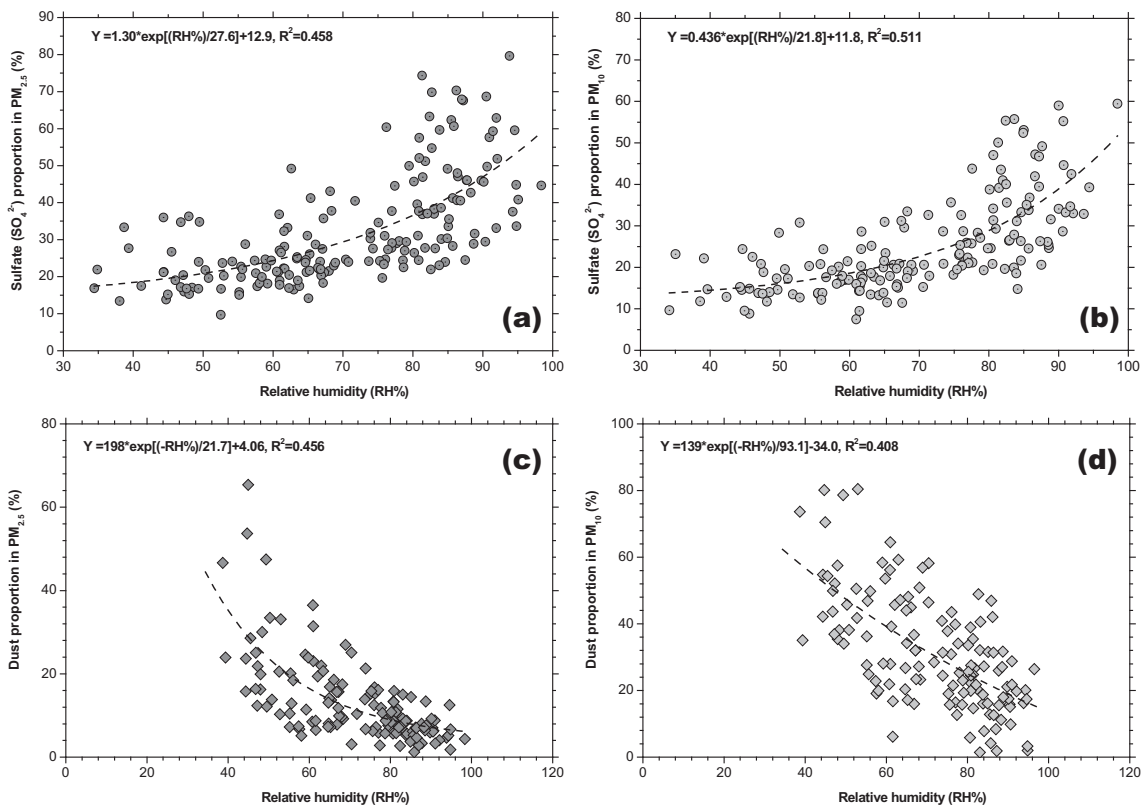


Fig. 5. The relationship between the sulfate (SO_4^{2-}) proportion in (a) $\text{PM}_{2.5}$ and (b) PM_{10} with the ambient relative humidity (RH) at BGS. (c), (d), same as (a), (b) but for the dust proportion.

organic carbon or soil material. Over this coastal area of China with frequently more humid weather, RH effects on the oxidation of the precursor gases and formation of sulfate/

nitrate and on the enhancement of aerosol extinction tend to be more important than the contribution from the mineral dust aerosol (which occasionally impacts this region in spring).

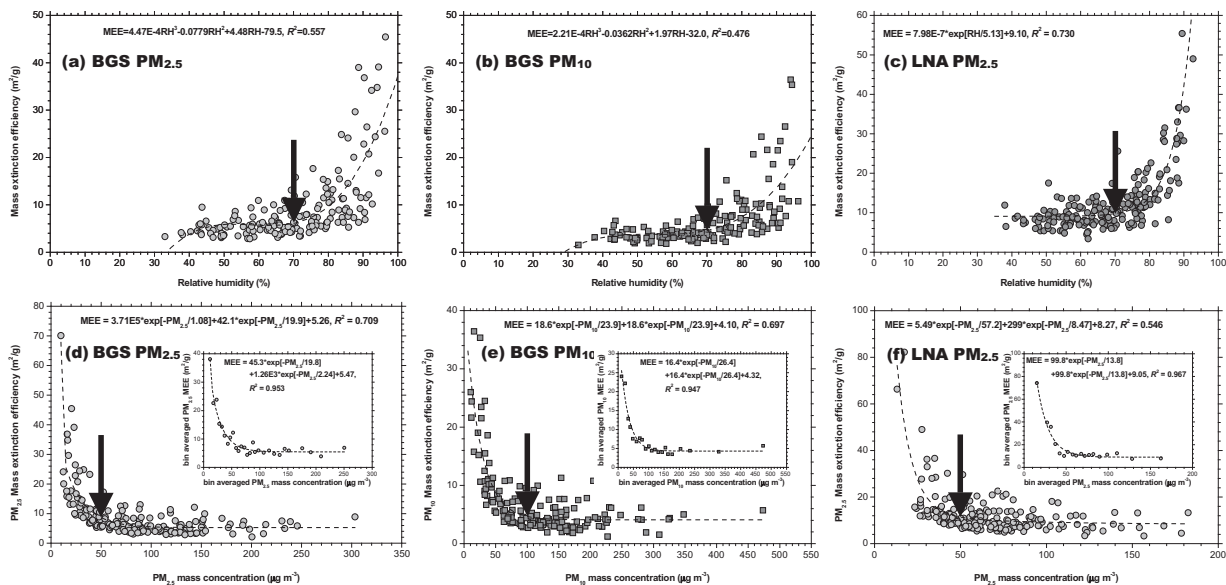


Fig. 6. The relationship between the mass extinction efficiency (MEE) of aerosol with (a) relative humidity (RH) and (d) $\text{PM}_{2.5}$ mass concentration at BGS; (b), (e), same as (a), (d) but for PM_{10} ; (c), (f), same as (a), (d) but for $\text{PM}_{2.5}$ at LNA. The insets on the upper right of Fig. 6d, e and f show corresponding relationship between the bin averaged variables. The thick black arrows in Fig. 6a, b and c (Fig. 6d, e and f) indicate the threshold value of RH (PM concentration); beyond the RH threshold (below the PM concentration threshold) MEE responds more efficiently with the increase of RH (PM concentration).

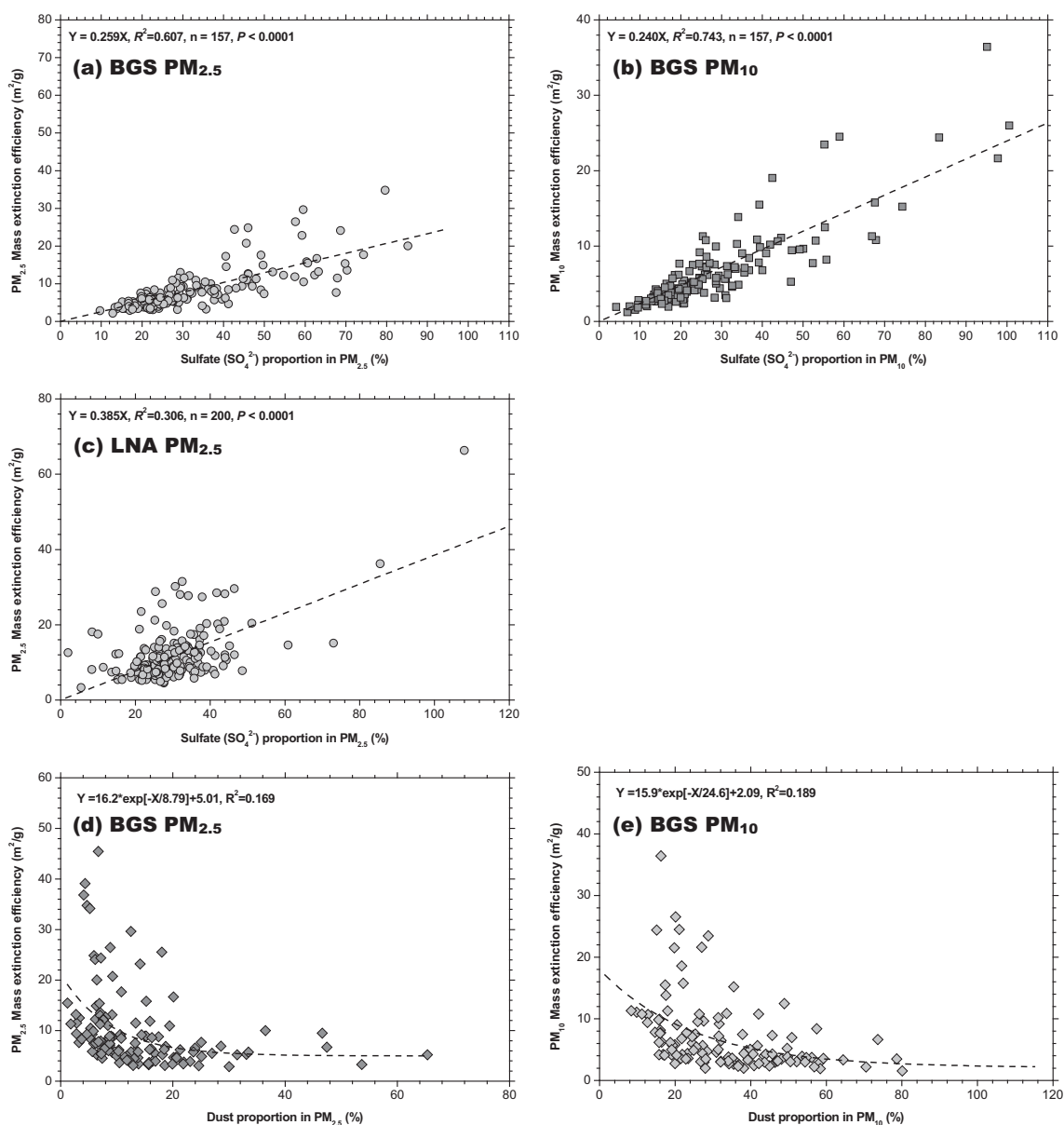


Fig. 7. The relationship between the mass extinction efficiency (MEE) of aerosol and sulfate (SO₄²⁻) proportion in (a) PM_{2.5} and (b) PM₁₀ at BGS; (c) same as (a) but for PM_{2.5} at LNA; (d), (e), same as (a), (b) but for dust proportion at BGS.

Note here the “significantly” higher MEE values in Fig. 6a, b and c are found to be associated with higher RH. In this study the MEE is calculated as the ratio of the extinction coefficient to the dry PM mass concentration. In the more humid environment, hygroscopic growth of the particles should contribute more efficiently to the ambient aerosol mass, thus the dry PM concentration should be much less than the ambient PM concentration, which might consequently result in the high MEE then.

3.5. Aerosol MEE and sulfate proportion for different transport clusters

Comparison between two categories of the backward trajectory clusters to BGS gets similar result. The trajectories

from the direction of ocean (clusters A, B, C, D and J) have average RH larger than 70% (76%–91%, Fig. 1 and Table 1), the sulfate proportions in PM are within 30%–41%, and MEE are within 6.8–20 m²/g. These values are greater than their counterparts for the trajectories from the continent (clusters E, F, G, H and I; RHs within 52%–67%, the sulfate proportions within 16%–19%, MEE within 3.2–4.6 m²/g). Especially, the two trajectory clusters only occurring in summer (B and C) are associated with higher temperature (28 °C and 25 °C), higher RH (81% and 91%), higher sulfate proportion (62% and 57% for PM_{2.5}, 41% and 38% for PM₁₀) and higher MEE in m²/g (13 and 27 for PM_{2.5}, 9.0 and 20 for PM₁₀). In summary, high (low) MEE occurs under the influence of humid (dry) airmass from the ocean (continent). This finding has important insights for Vis

Table 1
Contribution percentage of each trajectory cluster and the corresponding mean ambient temperature, relative humidity (RH), visibility as well as mass concentration, sulfate proportion and mass extinction efficiency (MEE) for PM_{2.5} and PM₁₀ at BGS.

Trajectory cluster	Proportion of all trajectories (%)				Temperature (°C)	RH (%)	Visibility (km)	Mean mass concentration (μg m ⁻³)		Sulfate (SO ₄ ²⁻) proportion (%)		MEE (m ² /g)		
	Spring	Summer	Autumn	Winter				Sum	PM _{2.5}	PM ₁₀	PM _{2.5}	PM ₁₀	PM _{2.5}	PM ₁₀
	35	67	40	15				40	89.5	120	40	36	12	9.1
A					19^a	78	6.8							
B		3.2			28	81	13	27.2	30.2	62	41	13	9.0	
C		3.4			25	91	8.3	20.6	24.8	57	38	27	20	
D	12		14	0.55	19	76	10	64.9	89.9	35	30	11	6.8	
E	2	0.25		4.1	2.6	64	11	69.0	124	27	17	7.0	4.0	
F	17	0.74	13	27	6.3	58	11	73.7	108	23	18	5.5	3.9	
G	2.3		1.9	4.7	3.9	52	12	61.0	102	27	16	7.5	4.1	
H	20	3.7	19	27	9.0	67	8.0	108	150	24	19	6.5	4.6	
I	9.3	0.25	12	21	5.5	59	10	89.9	139	21	16	5.2	3.2	
J	3	7.8			24	82	4.7	84.4	99.6	36	38	15	13	
Total					14	71	8.4	85.4	119	32	27	9.4	6.9	

^a Boldface indicates value of ambient temperature, RH, sulfate proportion and MEE of PM for trajectory clusters with mean RH > 70%.

variation over this region; that is, for the air mass from the ocean or from the direction of water vapor supply, considerable aerosol extinction is expected due to the enhanced formation of the secondary aerosol species, which is associated with Vis impairment.

Except for 27 m²/g of MEE for cluster J, the statistics of the PM_{2.5} MEE for the other trajectory clusters are within 5.2–15 m²/g, which are less than or comparable with the MEE reported for sulfate (15.6 or 15.7 m²/g) in previous studies (Pandolfi et al., 2011; Li et al., 2013). The cause of the “significantly” higher MEE (27 m²/g) associated with the highest RH (91%) for cluster J is similar as explained in the end of Section 3.4.

3.6. Roles of PM and RH in the Vis–MEE relationship

Vis shows exponential decay with the increase of MEE (Fig. 8). In the range with MEE > 30, the decrease of Vis is mainly controlled by the increase of PM concentration rather than by the increase of MEE (top panel). While in the range of MEE < 30, both the increase of MEE and increase of PM concentration contribute to Vis decline.

Colors in the bottom panel (Fig. 8) indicate bins of RH. In the range with MEE > 30, RH is generally larger than 85% and Vis less than 4 km, probably reflecting Vis decline during fog when hygroscopic growth plays an important role. In the range of MEE < 20, the points in different RH bins mix; decrease of Vis probably results from mixed effects, such as the increase of PM concentration, hygroscopic growth and other factors.

Finally, the mass (concentration) ratio between PM_{2.5} and PM₁₀ is 0.731 at BGS, while the MEE ratio between PM_{2.5} and PM₁₀ is 1.17; PM_{2.5} contribution to the extinction is thus about 86% (0.731 × 1.17). PM_{2.5} is the major contributor to the aerosol mass (73%) and extinction (also see Supplementary material 1).

3.7. Contribution of sulfate and nitrate to aerosol extinction

Using the IMPROVE (Interagency Monitoring of Protected Visual Environments) method (<http://vista.cira.colostate.edu/improve/Tools/ReconBext/reconBext.htm>), we reconstruct the extinction coefficient (B_{ext}) of sulfate and nitrate at BGS,

$$B_{\text{ext}}(\text{Mm}^{-1}) = 3f(\text{rh})[\text{Sulfate}] + 3f(\text{rh})[\text{Nitrate}] \quad (4)$$

where [Sulfate] and [Nitrate] are the mass concentrations calculated based on the forms of (NH₄)₂SO₄ and NH₄NO₃, and f(rh) is the relative humidity correction factor for converting dry extinction values to ambient extinction (http://vista.cira.colostate.edu/improve/Tools/humidity_correction.htm). Note here that the concentrations of organic matter and light-absorbing carbon are not measured in this study, and only the B_{ext} values of sulfate and nitrate are reconstructed using the IMPROVE method; while the total light extinction coefficient (total B_{ext}) is calculated according to formula (1) in Section 2.2.

Vis shows exponential decay accompanied with the increase of the B_{ext} of sulfate and nitrate (which can explain about 74% of the variance of Vis); increase of the sulfate and nitrate B_{ext} and decrease of Vis are generally associated with the increase of RH (Fig. 9a). The B_{ext} of sulfate and nitrate is

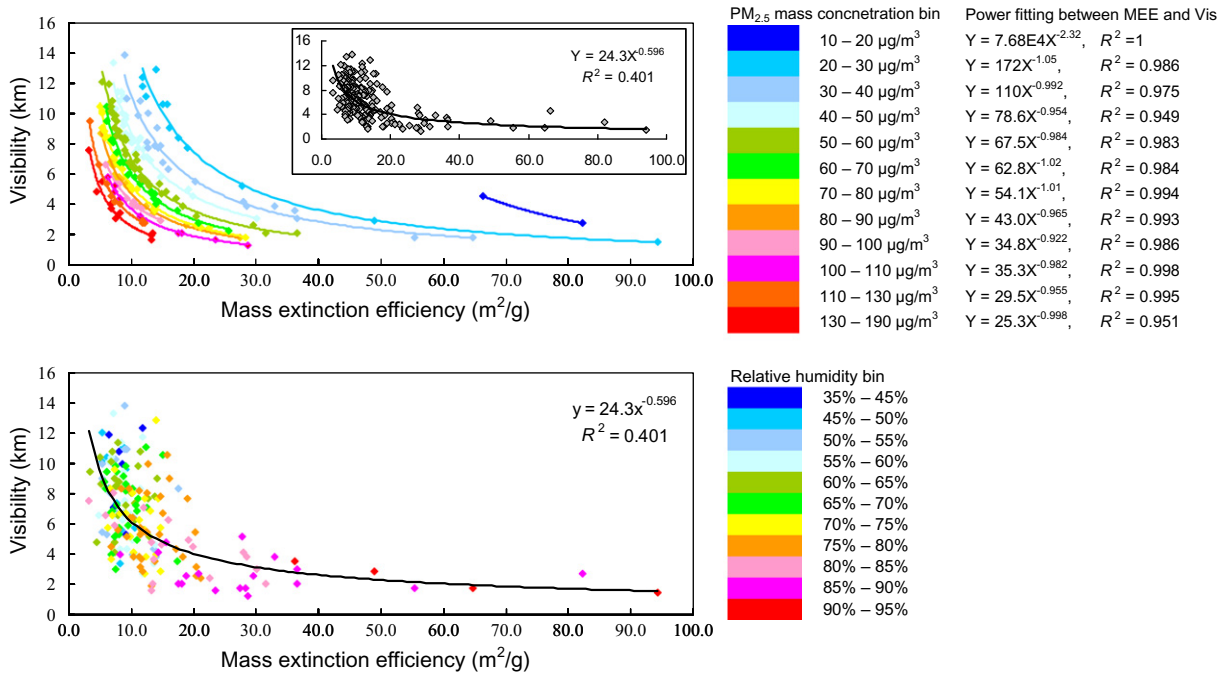


Fig. 8. The relationship between visibility (Vis) and mass extinction efficiency (MEE) for PM_{2.5} at LNA. (Top) Colors of the scatter points and fitting lines indicate the PM concentration bin; the upper right inset shows fitting between Vis and MEE for the whole dataset; fitting (and R²) for each bin is also presented at the right side. (Bottom) Colors of the scatter points indicate the relative humidity (RH) bin.

found to account for about 61% of the total B_{ext} at BGS (Fig. 9b), comparable with the result of Jung et al. (2009b) that sulfate and nitrate contribute to about 42.2% and 24.9% (respectively) to the light extinction in Beijing in summer 2006. These analyses suggest that sulfate and nitrate are major contributors to the light extinction and consequently Vis degradation in this coastal area of China.

4. Conclusion

The influence of RH on the chemical composition and light extinction of the aerosol at two sites in coastal area of China was examined in this study. Enhancement of the ambient aerosol extinction is found to be associated with the increase of the

mass fraction of sulfate and nitrate in PM when RH increases. The aerosol exhibits a cation deficit at both BGS and LNA, and higher aerosol acidity is associated with higher PM concentration, lower Vis and higher RH, suggesting that the more humid condition tends to be favorable for the formation of the pollution episodes associated with more acidic aerosol, probably due to increased contributions from sulfate and nitrate which resulted from more efficient oxidation of the precursor gases and formation of the secondary species and strengthened hygroscopic growth. Sulfate and nitrate are found to be the major contributors to the light extinction (about 61% at BGS) and Vis degradation over the coastal area of China. The contributions of sulfate and nitrate to light extinction (and Vis impairment) become more important at elevated RH. RH affects

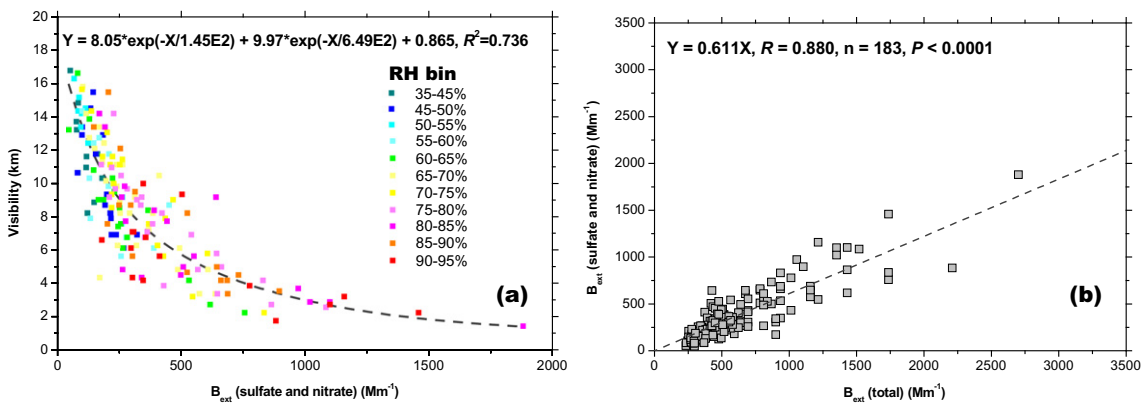


Fig. 9. (a) The relationship between visibility (Vis) and the extinction coefficient (B_{ext}) of sulfate and nitrate at BGS. (b) The relationship between the B_{ext} of sulfate and nitrate and the total B_{ext} at BGS.

the chemical composition of the aerosol and consequently alters its optical properties, which has important implications to Vis degradation over the region.

The hygroscopic species (sulfate and nitrate) and RH are found to be crucial factors contributing to Vis degradation. With hygroscopic growth in consideration, the RH corrected PM concentration shows better correlation with Vis than the dry PM concentration. As the precursor gases of sulfate and nitrate are at high concentration in ECN due to intensive emission, RH thus plays a key role in the oxidization of the precursor gases and formation of the secondary species as well as hygroscopic growth, its contribution to aerosol extinction and implications on the severe, frequent, long-durative and widespread haze and fog (Vis impairment) events over ECN should be considered (in addition to controlling of the emissions) in formulating strategies to improve air quality and Vis in the region.

Different from the general knowledge that the maritime origin airmass is always associated with fresh air and presumably high Vis, our results show that at BGS the airmasses from the ocean directions are associated with higher RH, higher sulfate mass fraction, higher MEE and consequently lower Vis compared with those from the continental directions. RH and water vapor supply strongly affect formation of the secondary hygroscopic aerosol species (such as sulfate and nitrate) and hygroscopic growth. The contrast in the aerosol extinction for the airmasses from the ocean and from the continent suggests that the aerosol optical properties varied under different circulation patterns, its influence on Vis degradation should be carefully considered.

The findings of this research are useful in study and predication of the low Vis events and regulation of the regional air pollution episodes. Future study on accurate parameterization of the ambient aerosol mixed by the hygroscopic species, dust and carbonaceous components based on in situ measurement is warranted to better understand optical properties of the aerosol and related Vis impairment over coastal China.

Acknowledgments

This research is supported by National Basic Research Program of China (2011CB403401), NSFC 41276009 and Chinese Ministry of Education's 111 Project (B07036).

Appendix A. Supplementary data

Supplementary data to this article can be found online at <http://dx.doi.org/10.1016/j.atmosres.2014.10.009>.

References

- Arimoto, R., Snow, J.A., Graustein, W.C., Moody, J.L., Ray, B.J., Duce, R.A., Turekian, K.K., Mering, H.B., 1999. Influences of atmospheric transport pathways on radionuclide activities in aerosol particles from over the North Atlantic. *J. Geophys. Res.* 104, 21301–21316.
- Bi, J.R., Huang, J.P., Hu, Z.Y., Holben, B.N., Guo, Z.Q., 2014. Investigate the aerosol optical and radiative characteristics of heavy haze episodes in Beijing during January of 2013. *J. Geophys. Res.* <http://dx.doi.org/10.1002/2014JD021757>.
- Chan, C.K., Yao, X.H., 2008. Air pollution in mega cities in China. *Atmos. Environ.* 42, 1–42.
- Chang, D., Song, Y., Liu, B., 2009a. Visibility trends in six megacities in China 1973–2007. *Atmos. Res.* 94, 161–167.
- Chang, D., Song, Y., Liu, B., 2009b. Visibility trends in six mega cities in China 1973–2007. *Atmos. Res.* 94, 161–167.
- Charlson, R.J., 1969. Atmospheric visibility related to aerosol mass concentration. *Environ. Sci. Technol.* 3, 913–918.
- Che, H., Zhang, X., Li, Y., Zhou, Z., Qu, J.J., 2007. Horizontal visibility trends in China 1981–2005. *Geophys. Res. Lett.* 34, L24706.
- China Meteorological Administration, 2003. Specifications for surface meteorological observation (in Chinese). China Meteorological Press, p. 151.
- China Meteorological Administration, 2010. Visibility grade and forecast (in Chinese). China Meteorological Press, p. 7.
- Chýlek, P., Videen, G., Ngo, D., Pinnick, R.G., Klett, J.D., 1995. Effect of black carbon on the optical properties and climate forcing of sulfate aerosols. *J. Geophys. Res.* 100 (D8), 16325–16332.
- Day, D.E., Malm, W.C., 2001. Aerosol light scattering measurements as a function of relative humidity: a comparison between measurements made at three different sites. *Atmos. Environ.* 35, 5169–5176.
- Deng, X.J., Tie, X.X., Wu, D., Zhou, X.J., Bi, X.Y., Tan, H.B., Li, F., Jiang, C.L., 2008. Long-term trend of visibility and its characterizations in the Pearl River Delta (PRD) region, China. *Atmos. Environ.* 42, 1424–1435.
- Draxler, R.R., Hess, G.D., 1998. An overview of the HYSPLIT_4 modeling system for trajectories, dispersion, and deposition. *Aust. Meteorol. Mag.* 47, 295–308.
- Eck, T.F., Holben, B.N., Reid, J.S., Sinyuk, A., Dubovik, O., Smirnov, A., Giles, D., O'Neill, N.T., Tsay, S.-C., Ji, Q., Mandoos, A.A., Khan, M.R., Reid, E.A., Schafer, J.S., Sorokine, M., Newcomb, W., Slutsker, I., 2008. Spatial and temporal variability of column-integrated aerosol optical properties in the southern Arabian Gulf and United Arab Emirates in summer. *J. Geophys. Res.* 113, D01204. <http://dx.doi.org/10.1029/2007JD008944>.
- Fan, Y.Q., Li, E.J., Fan, Z.L., 2005. Visibility trends in 11 cities of Hebei province during 1960–2002 (in Chinese with English abstract). *Chin. J. Atmos. Sci.* 29 (4), 526–535.
- Ge, C., Zhang, M.G., Zhu, L.Y., Han, X., Wang, J., 2011. Simulated seasonal variations in wet acid depositions over East Asia. *J. Air Waste Manage. Assoc.* 61, 1246–1261.
- Jain, M., Kulshrestha, U.C., Sarkar, A.K., Parashar, D.C., 2000. Influence of crustal aerosols on wet deposition at urban and rural sites in India. *Atmos. Environ.* 34, 5129–5137.
- Jung, J., Kim, Y.J., 2011. Tracking sources of severe haze episodes and their physicochemical and hygroscopic properties under Asian continental outflow: long-range transport pollution, postharvest biomass burning, and Asian dust. *J. Geophys. Res.* 116, D02206. <http://dx.doi.org/10.1029/2010JD014555>.
- Jung, J., Lee, H., Kim, Y.J., Liu, X., Zhang, Y., Gu, J., Fan, S., 2009a. Aerosol chemistry and the effect of aerosol water content on visibility impairment and radiative forcing in Guangzhou during the 2006 Pearl River Delta campaign. *J. Environ. Manag.* 90, 3231–3244.
- Jung, J., Lee, H., Kim, Y.J., Liu, X., Zhang, Y., Hu, M., Sugimoto, N., 2009b. Optical properties of atmospheric aerosols obtained by in situ and remote measurements during 2006 Campaign of Air Quality Research in Beijing (CARE Beijing–2006). *J. Geophys. Res.* 114, D00G02. <http://dx.doi.org/10.1029/2008JD010337>.
- Kasten, F., 1969. Visibility forecast in the phase of pre-condensation. *Tellus* 21 (5), 631–635.
- Kotchenruther, R.A., Hobbs, P.V., Hegg, D.A., 1999. Humidification factors for atmospheric aerosols off the mid-Atlantic coast of the United States. *J. Geophys. Res.* 104 (D2), 2239–2251.
- Krivacsy, Z., Molnar, A., 1998. Size distribution of ions in atmospheric aerosols. *Atmos. Res.* 46, 271–291.
- Li, L., Chen, J., Wang, L., Melluki, W., Zhou, H., 2013. Aerosol single scattering albedo affected by chemical composition: an investigation using CRDS combined with MARGA. *Atmos. Res.* 124, 149–157.
- Lin, F.M., Jiao, L., Sheng, K., Wu, Y.Y., 2004. Acid rain pollution and its origin of Hangzhou (in Chinese). *Environ. Monit. Manag. Technol.* 16 (3), 17–20.
- Malm, W.C., Sisler, J.F., Huffman, D., Eldred, R.A., Cahill, T.A., 1994. Spatial and seasonal trends in particle concentration and optical extinction in the United States. *J. Geophys. Res.* 99 (D1), 1347–1370.
- Maxwell-Meier, K., Weber, R., Song, C., Orsini, D., Ma, Y., Carmichael, G.R., Streets, D.G., 2004. Inorganic composition of fine particles in mixed mineral dust–pollution plumes observed from airborne measurements during ACE-Asia. *J. Geophys. Res.* 109, D19S07.
- Noll, K.E., Mueller, P.K., Imada, M., 1968. Visibility and aerosol concentration in urban air. *Atmos. Environ.* 2 (5), 465–475.
- Pandolfi, M., Cusack, M., Alastuey, A., Querol, X., 2011. Variability of aerosol optical properties in the Western Mediterranean Basin. *Atmos. Chem. Phys.* 11, 8189–8203.
- Pu, Y.F., Yang, J.L., 2000. Relationship of acidification of air aerosols with relative humidity and its contributions to the formation of acid rain (in Chinese). *Clim. Environ. Res.* 5 (3), 296–303.
- Qiu, J.H., Yang, L.Q., 2000. Variation characteristics of atmospheric aerosol optical depths and visibility in North China during 1980–1994. *Atmos. Environ.* 34, 603–609.
- Qu, W.J., Zhang, X.Y., Arimoto, R., Wang, D., Wang, Y.Q., Yan, L.W., Li, Y., 2008. Chemical composition of the background aerosol at two sites in southwestern

- and northwestern China: potential influences of regional transport. *Tellus* 60B, 657–673.
- Qu, W., Wang, J., Gao, S., Wu, T., 2013. Effect of the strengthened western Pacific subtropical high on summer visibility decrease over eastern China since 1973. *J. Geophys. Res.* 118, 7142–7156.
- Qu, W., Wang, J., Zhang, X., Yang, Z., Gao, S., 2014w. Effect of cold wave on winter visibility over eastern China. *J. Geophys. Res.* (revised version in review).
- Rastak, N., Silvergren, S., Zieger, P., Wideqvist, U., Ström, J., Svenningsson, B., Maturilli, M., Tesche, M., Ekman, A.M.L., Tunved, P., Riipinen, I., 2014. Seasonal variation of aerosol water uptake and its impact on the direct radiative effect at Ny-Ålesund, Svalbard. *Atmos. Chem. Phys. Discuss.* 14, 7067–7111.
- Seinfeld, J.H., Pandis, S.N., 2006. *Atmospheric Chemistry and Physics: From air Pollution to Climate Change*, Second Ed. John Wiley, New York, p. 1326.
- Si, F.Q., Liu, J.G., Xie, P.H., Zhang, Y.J., Liu, W.Q., Kuze, H., Liu, C., Lagrosas, N., Takeuchi, N., 2005. Determination of aerosol extinction coefficient and mass extinction efficiency by DOAS with a flashlight source. *Chin. Phys. Lett.* 32, 2360–2364.
- Smirnov, A., Holben, B.N., Dubovik, O., O'Neill, N.T., Eck, T.F., Westphal, D.L., Goroch, A.K., Pietras, C., Slutsker, I., 2002. Atmospheric aerosol optical properties in the Persian Gulf. *J. Atmos. Sci.* 59 (3), 620–634.
- Sun, J.Q., 1985. The relativity of relative humidity and visibility (in Chinese). *Acta Meteorol. Sin.* 43 (2), 230–234.
- Sun, Y.L., Wang, Z.F., Fu, P.Q., Jiang, Q., Yang, T., Li, J., Ge, X.L., 2013. The impact of relative humidity on aerosol composition and evolution processes during wintertime in Beijing, China. *Atmos. Environ.* 77, 927–934.
- Sun, Y., Jiang, Q., Wang, Z., Fu, P., Li, J., Yang, T., Yin, Y., 2014. Investigation of the sources and evolution processes of severe haze pollution in Beijing in January 2013. *J. Geophys. Res.* 119. <http://dx.doi.org/10.1002/2014JD021641>.
- Tan, J.H., Duan, J.C., Chen, D.H., Wang, X.H., Guo, S.J., Bi, X.H., Sheng, G.Y., He, K.B., Fu, J.M., 2009. Chemical characteristics of haze during summer and winter in Guangzhou. *Atmos. Res.* 94, 238–245.
- Tao, M., Chen, L., Su, L., Tao, J., 2012. Satellite observation of regional haze pollution over the North China Plain. *J. Geophys. Res.* 117, D12203.
- Wang, J., Martin, S.T., 2007. Satellite characterization of urban aerosols: importance of including hygroscopicity and mixing state in the retrieval algorithms. *J. Geophys. Res.* 112, D17203. <http://dx.doi.org/10.1029/2006JD008078>.
- Wang, J., Jacob, D.J., Martin, S.T., 2008. Sensitivity of sulfate direct climate forcing to the hysteresis of particle phase transitions. *J. Geophys. Res.* 113, D11207.
- Wang, K.C., Dickinson, R.E., Liang, S.L., 2009. Clear sky visibility has decreased over land globally from 1973 to 2007. *Science* 323, 1468–1470.
- Xue, L., Zhang, H.H., Yang, G.P., 2011. Characteristics and source analysis of atmospheric aerosol ions over the Yellow Sea and the Bohai Sea in spring (in Chinese). *Acta Sci. Circumst.* 31 (11), 2329–2335.
- Yoon, S.C., Kim, J.Y., 2006. Influences of relative humidity on aerosol optical properties and aerosol radiative forcing during ACE-Asia. *Atmos. Environ.* 40, 4328–4338.
- Zhang, X.Y., Cao, J.J., Li, L.M., Arimoto, R., Cheng, Y., Huebert, B., Wang, D., 2002. Characterization of atmospheric aerosol over XiAn in the South Margin of the Loess Plateau, China. *Atmos. Environ.* 36, 4189–4199.
- Zhang, X.Y., Gong, S.L., Arimoto, R., Shen, Z.X., Mei, F.M., Wang, D., Cheng, Y., 2003. Characterization and temporal variation of Asian dust aerosol from a site in the northern Chinese deserts. *J. Atmos. Chem.* 44, 241–257.
- Zhao, X.J., Zhao, P.S., Xu, J., Meng, W., Pu, W.W., Dong, F., He, D., Shi, Q.F., 2013. Analysis of a winter regional haze event and its formation mechanism in the North China Plain. *Atmos. Chem. Phys.* 13, 5685–5696.
- Zieger, P., Fierz-Schmidhauser, R., Weingartner, E., Baltensperger, U., 2013. Effects of relative humidity on aerosol light scattering: results from different European sites. *Atmos. Chem. Phys.* 13, 10609–10631. <http://dx.doi.org/10.5194/acp-13-10609-2013>.